Influence of the choice of insolation forcing on the results of a conceptual glacial cycle model

Gaëlle Leloup[1,2] and Didier Paillard[2]

[1]Agence Nationale pour la gestion des déchets radioactifs (ANDRA), 1 Rue Jean Monnet, 92290 Châtenay-Malabry, France
[2]Laboratoire des Sciences du Climat et de l'Environnement, LSCE/IPSL, CEA-CNRS-UVSQ-Université Paris-Saclay, 91198 Gif-sur-Yvette, France

Correspondence: Gaëlle Leloup (gaelle.leloup@lsce.ipsl.fr)

Abstract.

Over the Quaternary, the ice volume variations are "paced" by the astronomy. However, the precise way in which the astronomical parameters influence the glacial-interglacial cycles is not clear. The origin of the 100 kyr cycles over the last million year and of the switch from 40 kyr to 100 kyr cycles over the Mid Pleistocene Transition remain largely unexplained. By representing the climate system as oscillating between two states, glaciation and deglaciation, switching once a glaciation and a deglaciation thresholds are crossed, the main features of the ice volume record can be reproduced (Parrenin and Paillard, 2012). However, previous studies have only focused on the use of a single summer insolation as input. Here, we use a simple conceptual model to test and discuss the influence of the use of different summer insolation forcings, having different contributions from precession and obliquity, on the model results. We show that some features are robust. Specifically, to be able to reproduce the frequency shift over the Mid Pleistocene Transition, the deglaciation threshold needs to increase over time, independently of the summer insolation used as input. The quality of the model data agreement however depends on the chosen type of summer insolation and time period considered.

1 Introduction

Paleoclimate records over the Quaternary (last 2.6 Myr), such as ice cores (Jouzel et al., 2007) or marine cores (Lisiecki and Raymo, 2005) show a succession of oscillations. These oscillations are due to the build up and retreat of northern continental ice sheets, corresponding to respectively cold and warm periods known as the glacial - interglacial cycles.

Over the last million year, there is an alternance of long glaciations, followed by quick deglaciations leading to cycles of a period of 100 kyr. Yet, on the earliest part of the record, glacial-interglacial cycles are mostly dominated by a frequency of 41 kyr with lower amplitude. Spectral analysis of the record (Hays et al., 1976) have revealed that astronomical frequencies are imprinted into the ice volume record, suggesting a strong link between insolation and the glacial - interglacial cycles. However, the nature and physics of this link remain unclear. This has been a central question since the discovery of previous warm and cold periods, and long before the obtention of continuous $\delta^{18}O$ records. It is known that the variations of annual total energy are of too low amplitude to explain such changes (Croll, 1864). Therefore, focus has been set on seasonal variations. Croll (1864) assumed that glaciations were linked to colder winter. In contrast, Milankovitch popularized the idea that the decisive

25 element for glaciation was the presence of cold summers (Berger, 2021), due to reduced summer insolation, at latitudes typical of Northern Hemisphere ice sheets, 65° N. This also raises the question of what period should be defined as summer : a specific single day, like the summer solstice; the astronomical summer between the two equinoxes; or a fixed number of days around the solstice. This choice leads to slightly different forcings with different contributions from obliquity and precession.

The obtention of 100 kyr cycles is not possible with a linear theory like the one of Milankovitch (Hays et al., 1976; Imbrie

30 and Imbrie, 1980), and a form of non-linearity is needed. Indeed, there is no simple relation between insolation extrema and ice volume extrema. One of the largest deglaciation (termination V) occured when insolation variations were minimal. On the contrary, insolation variations where maximal at termination III, whereas the transition was rather small. In addition, the amplitude of summer insolation variations is maximum every 400 kyr, but this frequency is absent from the paleoclimatic records.

35 The 100 kyr cycles have been proposed to be linked to either eccentricity driven variations of precession (Raymo, 1997; Lisiecki, 2010), obliquity (Huybers and Wunsch, 2005; Liu et al., 2008), or both (Huybers, 2011; Parrenin and Paillard, 2012), to internal oscillations phase locked to the astronomical forcing (Saltzman et al., 1984; Paillard, 1998; Gildor and Tziperman, 2000; Tziperman et al., 2006), or to internal oscillations independant of the astronomical forcing (Saltzman and Sutera, 1987; Toggweiler, 2008). Additionally, the Mid Pleistocene Transition (MPT) and the switch from a 41 kyr dominated record to a

40 100 kyr one remains mostly unexplained.

Several models have been developed to try to solve these questions. Calder (1974) was the first to develop a simple conceptual model, linking insolation and ice volume variations. Imbrie and Imbrie (1980) also developed a conceptual model, where the rate of change was different in the case of a warming or cooling climate. Paillard (1998) developed the idea that the glacial-interglacial cycles can be seen as relaxation oscillations between multiple equilibria, like a glaciation and a deglaciation state.

45 It was suggested that the criteria to trigger a deglaciation depends on both, insolation and ice volume, whereas the insolation alone seems able to trigger a glaciation (Parrenin and Paillard, 2003). Here, we adapt and simplify the model of Parrenin and Paillard (2003) and extend it over the whole Quaternary.

One of the critical questions is to decide which insolation to use as input. In his work, Milankovitch used "caloric seasons" at 65° N, the half year with the more insolation. This was also the case in Calder's model, who used caloric seasons at 50° N as

50 input. Imbrie and Imbrie (1980) used the July insolation. The use of summer insolation gradually shifted towards the use of the summer solstice insolation, most probably as it is easier to compute thanks to the tables provided by Berger (1978) and allows to obtain better fits on the more recent part of the records (Paillard, 2015). More recently, Huybers (2006) suggested that the Integrated Summer Insolation (ISI) over a certain threshold could be more adapted, as it would more closely follow positive degree days, an important metric for ice sheet mass balance. Others have also used combinations of orbital parameters as a

55 forcing (Imbrie et al., 2011; Parrenin and Paillard, 2012). However, most models only use one type of insolation forcing and do not consider the influence of other insolation forcing on the model results.

In our work, we will consider several summer insolation forcings at 65° N (the summer solstice insolation, the caloric season, and the Integrated Summer Insolation over two different threshold values) in order to study their influence on the model results. These different summer insolation forcings have similar shape, but the respective contribution of obliquity and precession differ.

60 The different insolations have different performances in matching the data, depending on the time period considered. However, we show that some features are independent of the insolation forcing used as input. In particular, we are able to reproduce a switch from 41 kyr oscillations before the MPT to 100 kyr cycles afterwards in agreement with the records for all insolation forcings, by varying a single parameter : the deglaciation threshold V_0. This is similar to the results of Paillard (1998) who obtained a frequency shift on the glacial cycles by using a linearly increasing deglaciation threshold. This is also coherent with

65 the more recent results of Tzedakis et al. (2017), which demonstrated that the particular sequence of interglacials that happened over the Quaternary and the frequency shift from 41 to 100 kyr could be explained with a simple rule, taking into account a deglaciation threshold that increases over time, leading to 'skipped' insolation peaks and longer cycles.

2 Conceptual model and methods

2.1 Conceptual model

70 The model used in our study is an adapted and simplified version of the conceptual model of Parrenin and Paillard (2003). The aim of conceptual models is not to explicitly model and represent physical processes but rather to help us understand critical aspects of the climate system.

For the glacial-interglacial cycles, it is not a new idea that the climate system can be represented by relaxation oscillations between multiple equilibria, like a glaciation and a deglaciation state (Paillard, 1998; Parrenin and Paillard, 2003, 2012).

75 The climate system is represented by two distinct states of evolution : the "glaciation state" (g) and "deglaciation state" (d). The evolution of the ice volume in these two states is described by :

$$
\begin{cases}
(d)\ \frac{dv}{dt} = -\frac{I}{\tau_i} + \frac{1}{\tau_g} \\
\\
(g)\ \frac{dv}{dt} = -\frac{I}{\tau_i} - \frac{v}{\tau_d}
\end{cases}
\tag{1}
$$

where v represents the normalized ice volume. τ_i, τ_d and τ_g are time constants. I is the normalized summer insolation forcing

80 at 65° N, a typical latitude for Northern Hemisphere ice sheets. In comparison to the work of Parrenin and Paillard (2003), the insolation forcing used is not truncated and there is no contribution from the obliquity. The first term of Eq. (1) is related to the external insolation forcing and represents ice melting during boreal summer. When the insolation is above average, the ice sheet melts, whereas when the insolation is low enough, the ice sheet grows. The second term of Eq. (1) represents an evolution trend linked to the system state : a slow glaciation in (g) state and a rapid deglaciation in (d) state. The implicit assumption

85 is made that the global ice volume changes are mainly driven by the Northern Hemisphere ice sheet waning and waxing, as we focus on the effect of insolation changes at high northern latitudes. This is not a limiting assumption as data suggest much lower sea level variation due to the Antarctic ice sheet than the Northern Hemisphere ones over glacial-interglacial timescales. For example, the contribution of the Antarctic ice sheet to the ∼120 m Last Glacial Maximum sea level drop is estimated to be between 10 and 35 m sea level equivalent (Lambeck et al., 2014). Other effects like thermal expansion, small glaciers and

90 ice caps are estimated to be around 3 to 4 m sea level equivalent. Furthermore, it has been suggested (Jakob et al., 2020) that

the growth of larger Northern Hemisphere ice sheets since the start of the Quaternary and the associated sea level drop has a stabilizing effect on the East Antarctic ice sheet, as it limits its exposure to warm ocean waters.

A critical point is to define the criteria for the switch between the glaciation and deglaciation states. The importance of orbital forcing alone seems able to start a glaciation (Khodri et al., 2001; Ganopolski and Calov, 2011). Therefore, the condition to

95   switch from the deglaciation state to the glaciation state is based on insolation only : it is possible to enter deglaciation when the insolation becomes low enough. On the contrary, to enter the deglaciation state, both ice volume and insolation seem to play a role (Raymo, 1997; Parrenin and Paillard, 2003, 2012), as terminations occur after considerable build-up of ice sheet over the last million year. To represent the role of both ice volume and insolation in the triggering of deglaciations, the condition to switch from (g) to (d) state uses a linear combination of ice volume and insolation. The deglaciation is triggered when the

100   combination crosses a defined threshold V_0 : the deglaciation threshold. As in the work of Parrenin and Paillard (2003), this allows transitions to occur with moderate insolation when the ice volume is large enough and reciprocally.

$$
\begin{cases}
(d) \; to \; (g) \; : I < I_0 \\
\\
(g) \; to \; (d) \; : I + V > V_0
\end{cases}
\tag{2}
$$

The idea that the deglaciation threshold is linked to both, insolation and ice volume, is not new (Parrenin and Paillard, 2003, 2012), and is similar to the one developed by Tzedakis et al. (2017), where the threshold for a complete deglaciation

105   decreases with time as the system accumulates instability with ice sheets becoming more sensitive to insolation increase. As the ice sheet grows and extends to lower latitudes, the insolation needed to reach a negative mass balance decreases. This idea has been confirmed with modelling studies (Abe-Ouchi et al., 2013). Several reasons can explain this increase of instability over time : delayed bedrock rebound and exposure to higher temperature as the ice sheet sinks (Oerlemans, 1980; Pollard, 1982; Abe-Ouchi et al., 2013), increase in basal sliding as the ice sheet grows and the base becomes warmer, as more isolated from

110   the cold surface temperature (MacAyeal, 1992; Marshall and Clark, 2002), ice-sheet margins calving (Pollard, 1982), decrease of the ice sheet albedo due to either snow aging (Gallée et al., 1992) or increase of dust deposition as the ice sheet expands (Peltier and Marshall, 1995; Ganopolski and Calov, 2011), increase of atmospheric CO_2 due to release of deep ocean carbon when the Antarctic ice sheet extends over continental shelves (Paillard and Parrenin, 2004; Bouttes et al., 2012).

2.2 Summer insolation

115   The conceptual model defined previously uses summer insolation as input. It is therefore important to consider which insolation should be used. Insolation is usually taken at 65° N, a typical latitude for Northern Hemisphere ice sheets. Several articles have used the summer solstice daily insolation at 65° N as input insolation forcing (Paillard, 1998; Parrenin and Paillard, 2003). Others (Tzedakis et al., 2017) have used the caloric season, as defined by Milankovitch (1941), defined as the half year with the more insolation. It is also possible to use as input a linear combination of orbital parameters (Imbrie et al., 2011; Parrenin

120   and Paillard, 2012). Huybers (2006) also defined the Integrated Summer Insolation above a threshold.

Here, for the first time, we want to examine the effect of this choice on the dynamics of a conceptual model. We therefore

use four different summer insolation forcings, and compare the model results obtained with each of them. We use the summer solstice insolation, the caloric season, and the Integrated Summer Insolation (ISI) above two different thresholds (300 $W\ m^{-2}$ and 400 $W\ m^{-2}$).

125   These four insolation forcings differ slightly, and have different contributions from precession and obliquity, as can be seen in Fig. 1. For example, the summer solstice insolation has a low contribution from obliquity (41 kyr) compared to the caloric season, or the Integrated Summer Insolation above 300 $W\ m^{-2}$. The summer solstice insolation and the caloric season were computed using the Analyseries software (Paillard et al., 1996).
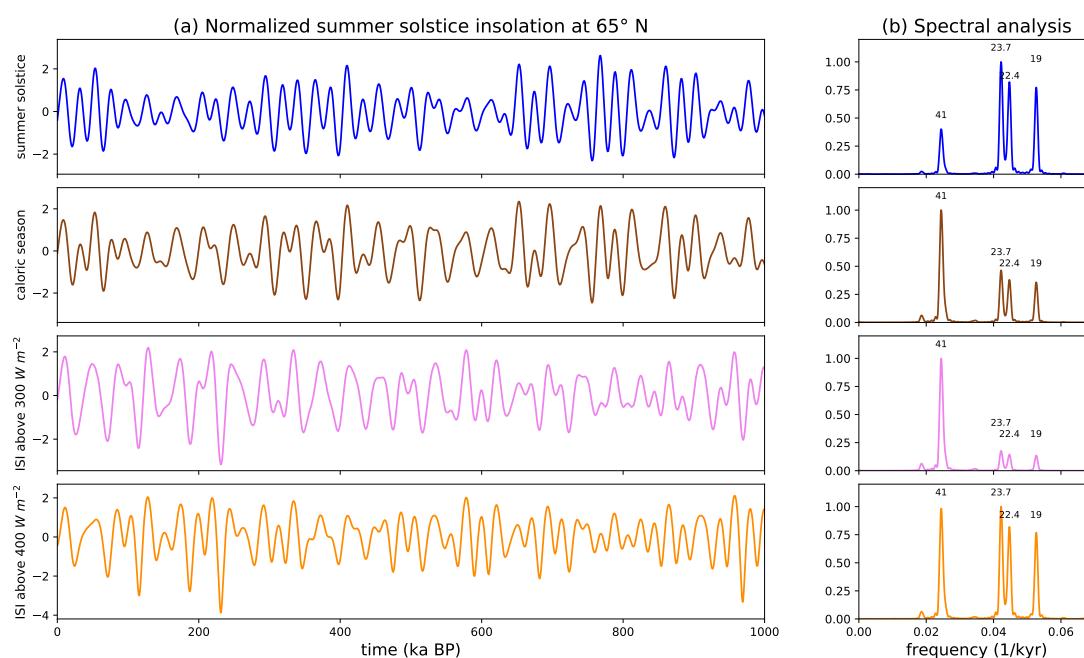
Figure 1. (a) The four different summer insolation forcings at 65° N (summer solstice, caloric season, Integrated Summer Insolation above 300 $W\ m^{-2}$ and above 400 $W\ m^{-2}$) displayed over the last million year (respectively in blue, brown, pink and orange). (b) Corresponding spectral analysis.

The Integrated Summer Insolation for a threshold τ (noted as ISI above τ or $ISI(\tau)$ in this article) was defined by Huybers

130   (2006) as the sum of the insolation on days exceeding this threshold.

$$ISI(\tau) = \sum_i \beta_i(W_i \cdot 86400)$$

Where W_i is the mean insolation of day i in $W\ m^{-2}$ and β_i equals one if $W_i > \tau$ and zero otherwise.

To compute the Integrated Summer Insolation $ISI(\tau)$, one first needs to compute the daily insolation on day i, and then sum

over the year for the days exceeding the threshold.

135 Here, we developed a Python code based on the Matlab code provided by Huybers (2006). Unlike the insolation files provided by Huybers (2006), which used the solution from Berger and Loutre (1991), we use the orbital parameters value the of the Laskar et al. (2004) solution for the calculation. This results in slightly different results for deeper time periods as the calculation of orbital parameters also differ with these two estimations.

2.3 Optimal model parameters.

140 The conceptual model relies on a small number of model parameters : τ_i, τ_g, τ_d and the two thresholds for the switch from a glaciation state to a deglaciation state and inversely : V_0 and I_0. For all the simulations performed, we kept τ_i = 9 kyr, τ_g = 30 kyr, τ_d = 12 kyr and I_0 = 0, as these parameters gave correct behaviour in previous studies (Parrenin and Paillard, 2003). No attempt was made to tune these parameters to have a behaviour closer to the data. On the contrary, more focus was set on the influence on the model results of the deglaciation threshold parameter, V_0. To compare our model results to data, we used the

145 benthic $\delta^{18}O$ stack "LR04" (Lisiecki and Raymo, 2005), considering that most of the $\delta^{18}O$ changes of benthic formainifera represent changes in continental ice (Shackleton, 1967; Shackleton and Opdyke, 1973).

The numerical integration of the model equations was performed with a fourth order Runge Kutta scheme. Several initial conditions with different initial ice volumes and state (glaciation and deglaciation) were tested, as well as several deglaciation thresholds V_0, in order to best fit the data.

150 To estimate which model parameters lead to model results closer to the data, the definition of an objective criteria is needed. The choice of such a criteria is not straightforward, and the use of different criteria, could have led to slightly different results. Our model is simple and does not aim at reproducing precisely the ice volume evolution, but rather at reproducing the main qualitative features, such as the shape and frequency of the oscillations. Therefore, we did not choose the correlation coefficient as a criteria, but developed our own one, based on the state of the system : glaciation or deglaciation. The definition of the

155 deglaciation state in the data is explained in Sect. 2.4. A critical point is that our model should be able to deglaciate at the right time, when a deglaciation is seen in the data. Conversely, the model should not produce deglaciation at periods where the data do not show deglaciation.

We defined a criteria for each of these two conditions, and assembled them in a global criteria. The deglaciations are considered as "missed" when, in the middle of the deglaciation in the data, the model has still not reached the deglaciation state. We simply

160 defined the criteria c_1 as the fraction of deglaciations correctly reproduced. This criteria equals to one when all the deglaciations take place at the right time, meaning that the model produces a deglaciation state every time a deglaciation is seen in the data.

To ensure that the model does not deglaciate too often, we looked at insolation maxima, that are not associated with deglaciation in the data and ensured the corresponding model state was glaciation. We decided to look specifically at insolation maxima, as it is where the model is the most likely to deglaciate when it should not. A deglaciation seen in the model at a place where

165 no deglaciation is seen in the data is considered as a "wrong transition". We defined the criteria c_2 as $c2 = 1 - w$, with w the fraction of wrong transitions. The c_2 criteria equals to one when the model does not deglaciate when it should not.

To take into account these two conditions, the overall accuracy criteria c is defined as $c = c_1 \cdot c_2$. It is equal to one when all the deglaciations are correctly placed and that no additional deglaciation compared to the data take place.

In order to study the evolution of the optimal model parameters over the Quaternary, it was divided into five 500 kyr periods. For each time periods, and insolation forcing considered, several simulations with different V_0 thresholds and initial conditions were carried out, and the parameter values maximizing the accuracy criteria c were selected.

2.4 Definition of the deglaciation state in the data

To calculate our accuracy criteria c and therefore determine the best fit parameters, a definition of the deglaciation in the data is needed. We based our definition on the interglacial classification developed by Tzedakis et al. (2017). Tzedakis et al. (2017) differentiates integlacials, continued interglacials and interstadials based on a detrended version of the LR04 (Lisiecki and Raymo, 2005) stack curve. A period is considered as an interglacial if its isotopic $\delta^{18}O$ is below a threshold (3.68 ‰). Two interglacials are considered as separated if separed by a local maximum above a threshold (3.92 ‰). This definition differs from the usual characterization of terminations, sometimes leading to several interglacials in the same isotopic stage.

The definition of Tzedakis et al. (2017) is for interglacials, and as our focus is not on interglacial periods but rather on deglaciations, we adapted it. We defined deglaciations as periods of decreasing $\delta^{18}O$ (and thus, ice volume, in our assumptions) preceeding the interglacials. The start of the deglaciation is taken as the last local maxima above the threshold of 3.92 ‰, and the end of the deglaciation is taken as the first local minima below the interglacial threshold of 3.68 ‰. The model state was compared to the middle of the deglaciation.

3 Results and discussion

3.1 Optimal deglaciation threshold V_0 and corresponding accuracy

The deglaciation threshold V_0 maximizing the accuracy for each of the five 500 kyr periods and insolation was computed. The results are displayed in Fig. 2.

In some cases, several values of the deglaciation threshold V_0 lead to the same accuracy criteria, whereas in other there is only one V_0 value maximizing the accuracy. When several V_0 values are equivalent, the mean value was plotted and the other possible values are represented with errorbars.

Over the same time periods, different insolation values lead to slightly different optimal V_0 threshold. But the most striking feature, is the increase of the optimal V_0 threshold over time, and more specifically for the last million year, after the Mid Pleistocene Transition. This feature is valid whatever the insolation type.

The corresponding accuracy criteria to the optimal V_0 threshold for each time period and insolation forcing is displayed in Fig. 3.

It is first noticeable, that the accuracy is higher on the last million year period, whatever the input summer insolation used. On the last million year, the summer solstice insolation as input produces the best results. However, this is not the case anymore
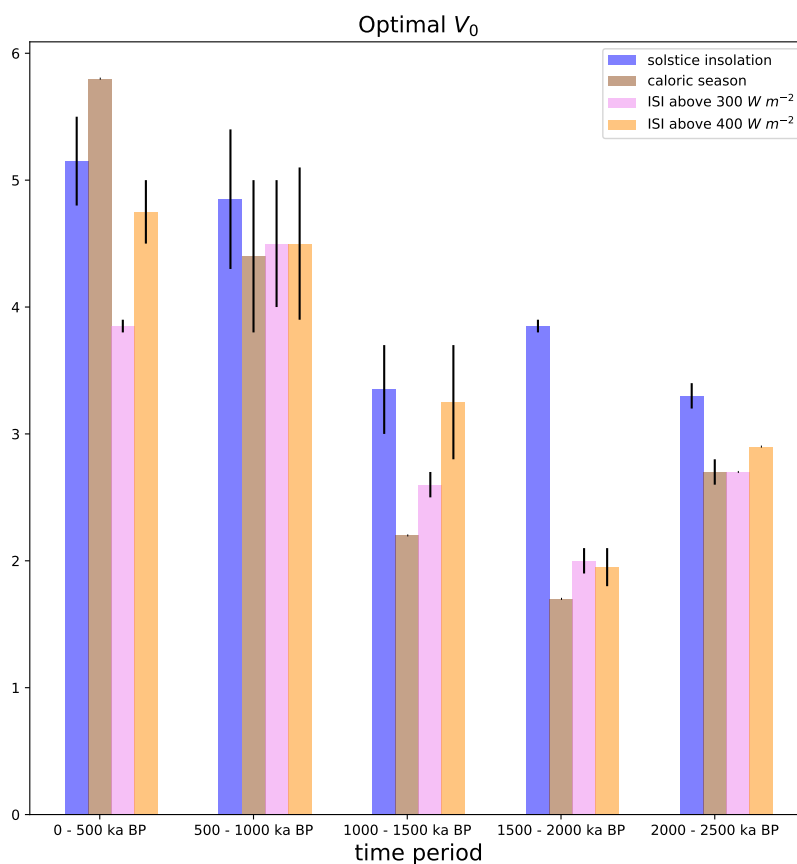
Figure 2. Optimal deglaciation threshold V_0 over the 5 different periods for the 4 different insolation forcings. When several values of the deglaciation threshold V_0 maximize the accuracy criteria, the mean value is plotted and the other possible values are represented with errorbars.

for more ancient time periods. On the contrary, the solstice insolation gives the worst results at the start of the Quaternary.

On the earlier part of the Quaternary (periods earlier than 1.5 Ma BP), the results are less robust. This is due to increased

200   incertainties in the LR04 record, and the associated definition of interglacial periods, which affects our accuracy criteria. In their classification, Tzedakis et al. (2017) stated that the definition of the valley depth needed to separate several interglacials was quite straighforward on the earlier part of the record, whereas for earlier time periods (ages older than 1.5 Ma BP), their method led to several "borderline cases", and that slighlty different choices for the interglacial and interstadial thresholds would have led to a different population of interglacial. For us, this would lead to a different definition of deglaciation, and thus a

205   different accuracy criteria. In addition, the resolution of the LR04 curve decreases with increasing age (Lisiecki and Raymo,
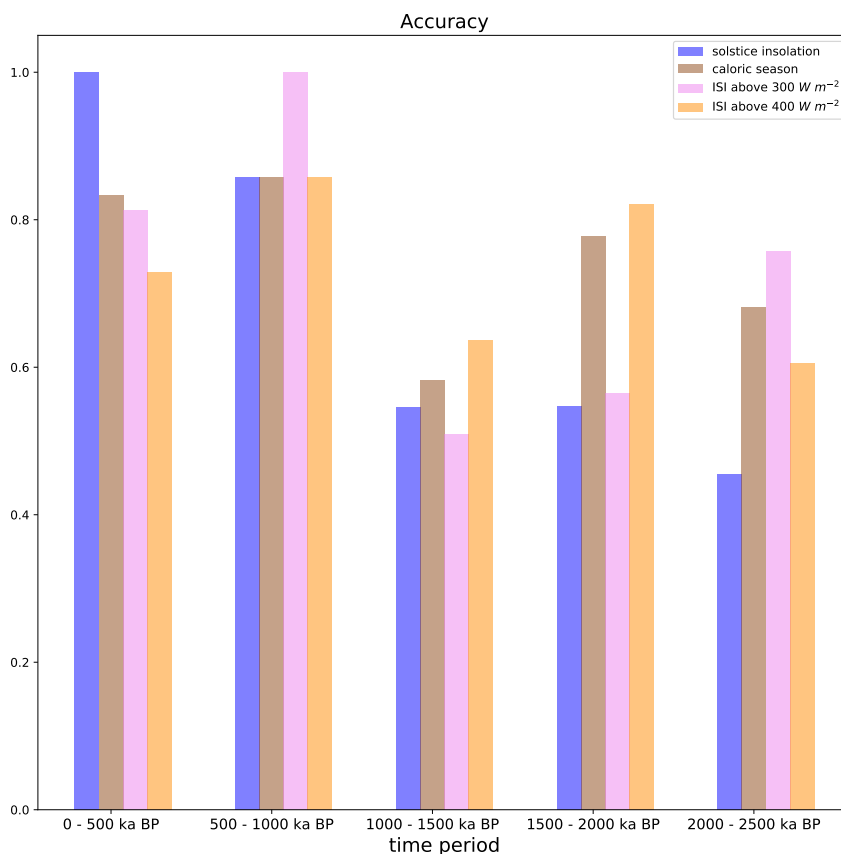
Figure 3. Accuracy over the 5 different periods for the 4 different insolation types.

2005), and for periods with lower resolution or more uncertain age matching, the amplitude of the peaks might be reduced (Tzedakis et al., 2017).

Moreover, the $\delta^{18}O$ LR04 curve includes at the same time an ice volume and deep water temperature component, and its use as an ice volume proxy has already been largely debated (Shackleton, 1967; Chappell and Shackleton, 1986; Shackleton and

210 Opdyke, 1973; Clark et al., 2006) and recent studies (Elderfield et al., 2012) have shown that the temperature component may be as large as 50%. All these reasons encourage us to remain at a qualitative level to fit the data.

The increase in the optimal deglaciation threshold V_0 over the MPT is however a robust feature, that does not depend on the input summer insolation forcing used. This is coherent with the work of Paillard (1998) and Tzedakis et al. (2017) who obtained a frequency shift from 41 kyr cycles to 100 kyr cycles with an increasing deglaciation threshold. Classical hypothesis

215 and possible physical meanings of the rise of the V_0 threshold often imply a gradual cooling, due to lower pCO_2 (Raymo, 1997; Paillard, 1998; Berger, 1978), but this idea is not supported by more recent data, which do not show a gradual decrease in pCO_2 trend, but rather only a decrease in minimal pCO_2 values (Hönisch et al., 2009; Yan et al., 2019). Other hypothesis

imply a gradual erosion of a thick regolith layer, that exposed the ice sheet to a higher friction bedrock allowing thicker ice sheet to develop (Clark and Pollard, 1998; Clark et al., 2006), or sea ice switching mechanism (Gildor and Tziperman, 2000).

220   The overall lowest accuracy on the more ancient part of the record suggests that our non linear threshold model is less adapted for this time period. Indeed, the ice volume might respond more linearly to the insolation forcing before the MPT, as some studies suggest (Tziperman and Gildor, 2003; Raymo and Nisancioglu, 2003). In contrast, others (Ashkenazy and Tziperman, 2004) have shown that the 41 kyr pre MPT oscillations are in fact significantly asymetric and therefore suggested that oscillations both before and after the MPT could be explained as self sustained variability of the climate system, phase

225   locked to the astronomical forcing. In our model, the deglaciation threshold V_0 changes over time leading to an amplitude change of the cycles. However, it cannot be excluded that the mechanisms behind the pre and post MPT glacial cycles are structurally different, and that they cannot be explained with the same physics and the same equations in our model. Moreover, this kind of conceptual model has mainly been constructed in order to explain the non linear feature of the 100 ka cycles, and it is therefore not surprising that its agreement with the data on the pre MPT period is less satisfying.

230   3.2 Best fit over the Quaternary

Our conceptual model is able to reproduce qualitatively well the data over the whole Quaternary. More specifically, its best guess for each summer insolation forcing (displayed in Fig. 4) is able to reproduce the frequency shift from a dominant 41 kyr period before 1 Ma BP to a dominant 100 kyr frequency afterwards observed in the data, and thus by varrying only one parameter during the whole simulation length : the deglaciation threshold V_0. The spectral analysis of the model outputs

235   exhibits a pattern similar to the spectral analysis of the LR04 curve. On the first part of the Quaternary (2.6 Ma BP to 1 Ma BP), the spectral analysis of the data is dominated by a 41 kyr (obliquity) peak. It is also the case for the model results, for each type of insolation. On the last million year, additionnaly to a 41 kyr peak, the spectral analysis of the data reveals a $\sim$ 100 kyr peak. It is also the case in the model output, for each type of insolation. Some differences are however noticeable. On the first part of the Quaternary, the model outputs also show a precession component (19 to 23 kyr), especially for the summer solstice

240   and the Integrated Summer Insolation above 400 $W\ m^{-2}$ forcings, which is not visible on the record. On the last million year, the lowest frequency peak appearing in the results slighlty varries (from $\sim$85 kyr peak for the Integrated Summer Insolation above 300 $W\ m^{-2}$ to $\sim$100 kyr peak for the summer solstice insolation). Compared to the data, all the model outputs have a more pronounced obliquity and precession component and a less pronounced 100 kyr component. In addition, model results for the summer solstice insolation and the caloric season forcings exhibit a secondary peak at period around 200 kyr, that does

245   not exist in the data. Like the previous model of Parrenin and Paillard (2003) frow which our model is adapted, we are able to obtain $\sim$ 100 kyr cycles without extracting 400 kyr, which is coherent with the record. Also similarly to their model, ours looses quicky its sensitivity to the initial conditions (after no more than 200 kyr).

Although our model reproduces qualitatively well the feature of the record, there are some noticeable model data mismatch that occur for all insolation type, around 1100 ka BP and 2030 ka BP. The amplitude of the oscillations produced is slightly too

250   high on the more ancient part of the Quaternary, especially when the Integrated Summer Insolation over 300 $W\ m^{-2}$ is used.
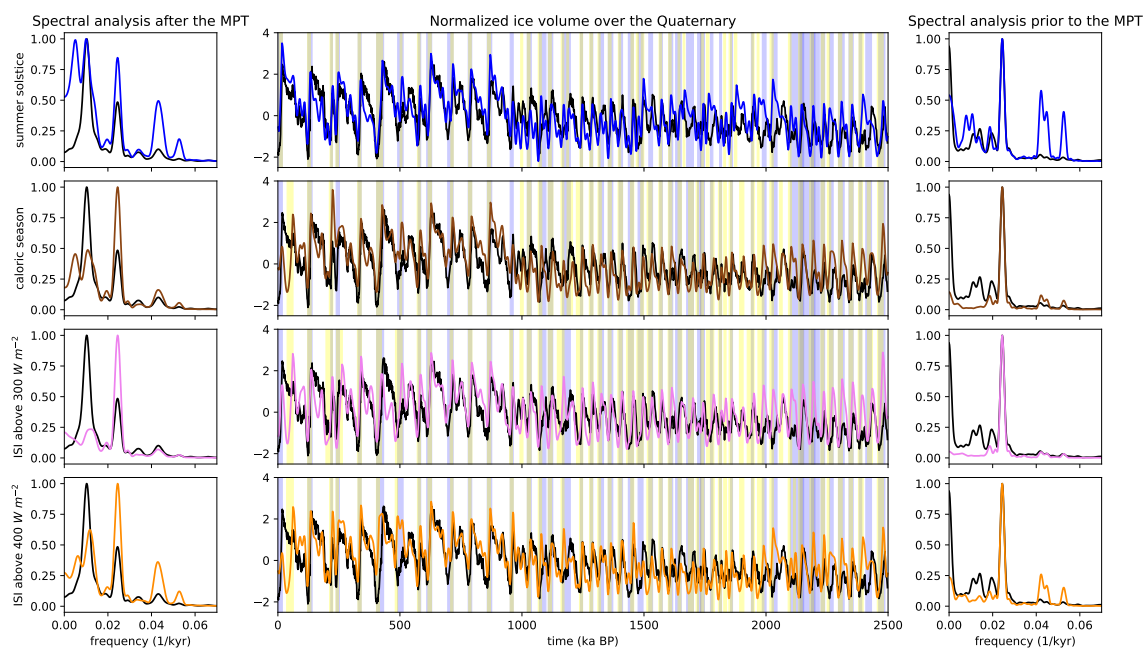
Figure 4. Best model fit over the whole Quaternary and corresponding spectral analysis. The middle panel represents the best fit of the model for the different summer insolation used as input, compared to the data. The results for the summer solstice insolation, caloric season, Integrated Summer Insolation above 300 $W\ m^{-2}$ and 400 $W\ m^{-2}$ are respectively displayed in blue, brown, pink and orange. The data (normalized LR04 curve) are in black. The blue shading represents deglaciation periods in the model and the yellow shading deglaciation periods in the data. This results in a green shading when deglaciations are seen in the model and data at the same time. The left panel represents the spectral analysis of the best fit solution over the last million year. The right panel represents the spectral analysis over the more ancient part of the Quaternary (before 1 Ma BP).

On the oldest part of the Quaternary, the caloric season forcing and the Integrated Summer Insolation over 300 $W\ m^{-2}$ seem to perform better in reproducing the frequency of the oscillations than the summer solstice insolation and Integrated Summer Insolation over 400 $W\ m^{-2}$. They correspond to the forcing with the strongest obliquity (41 kyr) component, which might explain why they more successfully represent this part of the record, that is dominated by obliquity.

255 Over the last million year, the highest accuracy is obtained with the summer solstice insolation as input forcing ($c = 0.92$ for the summer solstice insolation, $c = 0.82$ for the caloric season and Integrated Summer Insolation above 400 $W\ m^{-2}$ and $c = 0.87$ for the Integrated Summer Insolation above 300 $W\ m^{-2}$). However, this is mainly due to the fact that for the three other forcings (caloric season and Integrated Summer Insolation above 300 $W\ m^{-2}$ and 400 $W\ m^{-2}$), the last deglaciation occurs one insolation peak too early, around 50 ka BP. However, if one computes the accuracy over the last million year excluding the

260 last 100 kyr (period from 100 ka to 1000 ka BP), the accuracy is similar for all four forcings (0.92 for summer solstice, caloric season and ISI above 400 $W\ m^{-2}$ and 0.89 for ISI above 300 $W\ m^{-2}$).

Figure 5 displays two different alternatives. For the first one (full line), the optimal V_0 is calibrated over the [100 - 1000] ka BP period and maintained for the whole simulation ($V_0 = 5.0$ for the summer solstice insolation, 4.5 for the caloric season, 4.0 for the Integrated Summer Insolation above 300 $W\ m^{-2}$ and 4.6 for the Integrated Summer Insolation above 400 $W\ m^{-2}$).

265 Except with the summer solstice insolation as input, the three other insolation forcings fail to reproduce accurately the last deglaciation, as the last deglaciation occurs one insolation peak too early. The second alternative (dashed line) is to raise the deglaciation threshold V_0 over the last cycle (raised to $V_0 =5.5$ from 100 ka BP onward). In this case, the model does reproduce accurately the last deglaciation for all insolation forcings. This suggest, that we might need to raise further the V_0 threshold in order to model a theoretical "natural" future (without anthropogenic influence) with longer cycles. A cycle is not enough to

270 conclude on a trend, but this should be envisaged for future natural scenarios. This is coherent with the idea of Paillard (1998) who used a linearly increasing deglaciation threshold over the Quaternary.

3.3 Reflexions about the future

To model future natural evolutions of the climate system, one would need to take into account for possible evolutions of the V_0 threshold. In addition, one should consider different I_0 thresholds. The fate of the next kyrs in a natural scenario cannot

275 be ascertained with our conceptual model. Indeed, it depends on the onset (or not) of a glaciation, which is determined by the I_0 parameter. In our model, a broad range of I_0 parameter values lead to satisfying results over the last million year. These different values projected into the future either lead in one case to a glaciation start at present, and in the other case in a continued deglaciation, switching to a glaciation state only around 50 kyr after present at the next insolation minima. This is due to the current particular astronomical configuration, with a very low eccentricity, which leads to high summer insolation

280 minima, where the threshold for glaciation might not be reached. This is coherent with previous studies (Berger and Loutre, 2002; Paillard, 2001) which suggested that without anthropogenic forcing, the present interglacial might have lasted 50 kyrs. However, this exercise is purely academic, as we are not taking into account the role of anthropogenic CO_2, which would affect the glaciation and deglaciation thresholds (Archer and Ganopolski, 2005). Furthermore, our conceptual model cannot be extended outside the Quaternary, as the ice volume variations considered are exclusively the Northern Hemisphere one, and

285 our model is, by construction unable to represent projected future Antarctic ice sheet mass loss.

4 Conclusions

We have used a conceptual model with very few tunable parameters that represents the climatic system by multiple equilibria and relaxation oscillation. We used different summer insolation as input for our conceptual model : the summer solstice insolation, the caloric season, and the Integrated Summer Insolation over two different thresholds. With all these forcings, that have

290 different contributions from obliquity and precession, we are able to reproduce the feature of the ice volume over the whole Quaternary. More specifically, we are able to represent the Mid Pleistocene Transition and the switch from a 41 kyr dominated
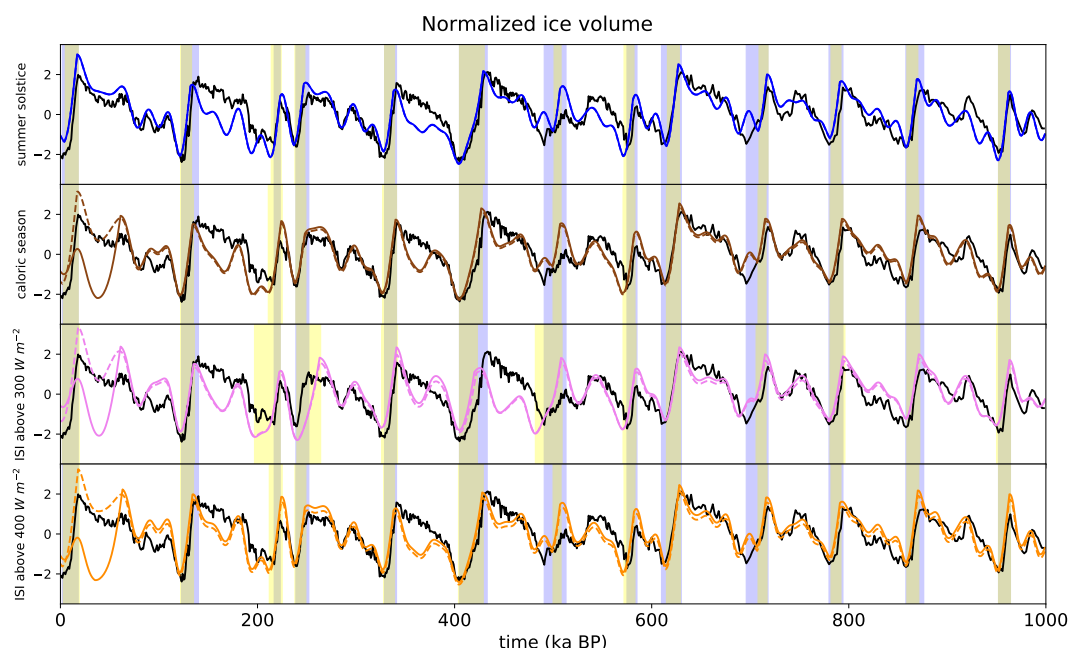
Figure 5. Normalized model results over the last million year, with the different summer insolation forcings : insolation at the summer solstice (blue), caloric season (brown), Integrated Summer Insolation over $300\ W\ m^{-2}$ (pink), and over $400\ W\ m^{-2}$ (orange). The full line is the best fit computed over the 100 - 1000 ka BP period. The dashed line represents the same solution, but with an increased V_0 threshold for the last deglaciation. The data (LR04 stack curve normalized) are in black. The blue shading represents deglaciation periods in the model (case of the increased V_0 threshold) and the yellow shading represents deglaciation periods in the data. This results in a green shading when deglaciations are seen in the model and data at the same time.

record to a 100 kyr dominated record, by raising the deglaciation threshold. This raise in the deglaciation threshold is valid regardless of the type of summer insolation forcing used as input. However, the data agreement is less satisfying before the MPT. This suggests the possibility that climate mechanisms might be structurally different before and after the MPT, with a
295 more linear behaviour in pre-MPT conditions. This highlights that models are designed to answer rather specific questions, and a model built specifically to explain 100 kyr cycles might be less efficient in a more linear setting. More generally, this kind of glacial-interglacial conceptual model is designed to explain the main features of the Quaternary time period characterized by the waning and waxing of Northern Hemisphere ice sheets under the influence of changing astronomical parameters. It is therefore unlikely to be directly applicable in a more general context, like the Pliocene and earlier periods, or in the context of
300 future climates under the long-term persistence of anthropogenic CO_2 (Archer and Ganopolski, 2005; Talento and Ganopolski, in review, 2021). In order to tackle such questions, it would be critical to gain a deeper understanding of the natural evolution of the other forcings involved in the climate system and most notably of the dynamics of the carbon cycle. Conceptual models

are likely to pave the way in this direction (Paillard, 2017). Indeed, just as in the case of the Quaternary, a full mechanistic simulation of the many processes at work is currently out of reach and the modelling work can only be very exploratory. Here, we have shown that some robust features are required to explain Quaternary ice age cycles. Similar conceptual modelling on a wider temporal scope over the Cenozoïc could help better understand the connections between the astronomical forcing, the carbon cycle, ice sheets and climate. This would help us imagine what the Anthropocene might be like.

Code and data availability. The model code as well as the insolation input files, spectral analysis and code needed to reproduce the figures are available for download online : https://doi.org/10.5281/zenodo.5458785

Author contributions. GL and DP designed the study. GL performed the simulations, and wrote the manuscript under the supervision of DP.

Competing interests. The authors declare that they have no conflict of interest.

Acknowledgements. The authors acknowledge the use of the LSCE storage and computing facilities.

References

Abe-Ouchi, A., Saito, F., Kawamura, K., Raymo, M., Okuno, J., Takahashi, K., and Blatter, H.: Insolation-driven 100,000-year glacial cycles
and hysteresis of ice-sheet volume, Nature, 500, 190–193, https://doi.org/10.1038/nature12374, 2013.

Archer, D. and Ganopolski, A.: A movable trigger: Fossil fuel CO_2 and the onset of the next glaciation, Geochem. Geophy. Geosy., 6,
https://doi.org/10.1029/2004GC000891, 2005.

Ashkenazy, Y. and Tziperman, E.: Are the 41 kyr glacial oscillations a linear response to Milankovitch forcing?, Quaternary Sci. Rev., 23,
1879–1890, https://doi.org/10.1016/j.quascirev.2004.04.008, 2004.

Berger, A.: Long-term variations of daily insolation and Quaternary climatic changes, J. Atmos. Sci., 35, 2362–2367, 1978.

Berger, A.: Milankovitch, the father of paleoclimate modeling, Clim. Past, 17, 1727–1733, https://doi.org/10.5194/cp-17-1727-2021, 2021.

Berger, A. and Loutre, M.-F.: Insolation values for the climate of the last 10 million years, Quaternary Sci. Rev., 10, 297–317,
https://doi.org/10.1016/0277-3791(91)90033-Q, 1991.

Berger, A. and Loutre, M.-F.: Climate: An Exceptionally Long Interglacial Ahead?, Science, 297, 1287–1288,
https://doi.org/10.1126/science.1076120, 2002.

Bouttes, N., Paillard, D., Roche, D. M., Waelbroeck, C., Kageyama, M., Lourantou, A., Michel, E., and Bopp, L.: Impact of oceanic processes
on the carbon cycle during the last termination, Clim. Past, 8, 149–170, https://doi.org/10.5194/cp-8-149-2012, 2012.

Calder, N.: Arithmetic of ice ages, Nature, 252, 216–218, https://doi.org/10.1038/252216a0, 1974.

Chappell, J. and Shackleton, N. J.: Oxygen isotopes and sea level, Nature, 324, 137–140, 1986.

Clark, P. and Pollard, D.: Origin of the Middle Pleistocene Transition by ice sheet erosion of regolith, Paleoceanography, 13, 1–9,
https://doi.org/10.1029/97PA02660, 1998.

Clark, P., Archer, D., Pollard, D., Blum, J. D., Rial, J., Brovkin, V., Mix, A., Pisias, N., and Roy, M.: The middle Pleistocene transi-
tion: characteristics, mechanisms, and implications for long-term changes in atmospheric pCO_2, Quaternary Sci. Rev., 25, 3150–3184,
https://doi.org/10.1016/j.quascirev.2006.07.008, 2006.

Croll, J.: XIII. On the physical cause of the change of climate during geological epochs, The London, Edinburgh, and Dublin Philosophical
Magazine and Journal of Science, 28, 121–137, https://doi.org/10.1080/14786446408643733, 1864.

Elderfield, H., Ferretti, P., Greaves, M., Crowhurst, S., Mccave, I. N., Hodell, D., and Piotrowski, A. M.: Evolution of Ocean Temperature
and Ice Volume Through the Mid-Pleistocene Climate Transition, Science, 337, 704–9, https://doi.org/10.1126/science.1221294, 2012.

Gallée, H., Van Yperselb, J. P., Fichefet, T., Marsiat, I., Tricot, C., and Berger, A.: Simulation of the last glacial cycle by a coupled, sec-
torially averaged climate-ice sheet model: 2. Response to insolation and CO_2 variations, J. Geophys. Res-atmos., 97, 15 713–15 740,
https://doi.org/10.1029/92JD01256, 1992.

Ganopolski, A. and Calov, R.: The role of orbital forcing, carbon dioxide and regolith in 100 kyr glacial cycles, Clim. Past, 7, 1415–1425,
https://doi.org/10.5194/cp-7-1415-2011, 2011.

Gildor, H. and Tziperman, E.: Sea ice as the glacial cycles' Climate switch: role of seasonal and orbital forcing, Paleoceanography, 15,
605–615, https://doi.org/10.1029/1999PA000461, 2000.

Hays, J., Imbrie, J., and Shackleton, N. J.: Variations in the Earth's Orbit: Pacemaker of the Ice Ages, Science, 194, 1121–1132,
https://doi.org/10.1126/science.194.4270.1121, 1976.

Hönisch, B., Hemming, N. G., Archer, D., Siddall, M., and McManus, J. F.: Atmospheric Carbon Dioxide Concentration Across the Mid-
Pleistocene Transition, Science, 324, 1551–1554, https://doi.org/10.1126/science.1171477, 2009.

350 Huybers, P.: Early Pleistocene glacial cycles and the integrated summer insolation forcing, Science, 313, 508–511, https://doi.org/10.1126/science.1125249, 2006.

Huybers, P.: Combined obliquity and precession pacing of late Pleistocene deglaciations, Nature, 480, 229–32, https://doi.org/10.1038/nature10626, 2011.

Huybers, P. and Wunsch, C.: Obliquity pacing of the late Pleistocene glacial terminations, Nature, 434, 491–494,
355 https://doi.org/10.1038/nature03401, 2005.

Imbrie, J. and Imbrie, J. Z.: Modeling the Climatic Response to Orbital Variations, Science, 207, 943–953, https://doi.org/10.1126/science.207.4434.943, 1980.

Imbrie, J. Z., Imbrie-Moore, A., and Lisiecki, L. E.: A phase-space model for Pleistocene ice volume, Earth Planet. Sc. Lett., 307, 94–102, 2011.

360 Jakob, K. A., Wilson, P. A., Pross, J., Ezard, T. H. G., Fiebig, J., Repschläger, J., and Friedrich, O.: A new sea-level record for the Neogene/Quaternary boundary reveals transition to a more stable East Antarctic Ice Sheet, P. Natl. Acad. Sci. USA, 117, 30 980–30 987, https://doi.org/10.1073/pnas.2004209117, 2020.

Jouzel, J., Masson-Delmotte, V., Cattani, O., Dreyfus, G., Falourd, S., Hoffmann, G., Minster, B., Nouet, J., Barnola, J., Chappellaz, J., Fischer, H., Gallet, J.-C., Johnsen, S., Leuenberger, M., Loulergue, L., Lüthi, D., Oerter, H., Parrenin, F., Raisbeck, G., and Wolff, E.: Orbital
365 and Millennial Antarctic Climate Variability over the Past 800,000 Years, Science, 317, 793–796, https://doi.org/10.1126/science.1141038, 2007.

Khodri, M., Leclainche, Y., Ramstein, G., Braconnot, P., Marti, O., and Cortijo, E.: Simulating the amplification of orbital forcing by ocean feedbacks in the last glaciation, Nature, 410, 570–574, 2001.

Lambeck, K., Rouby, H., Purcell, A., Sun, Y., and Sambridge, M.: Sea level and global ice volumes from the Last Glacial Maximum to the
370 Holocene, P. Natl. Acad. Sci. USA, 111, 15 296–15 303, https://doi.org/10.1073/pnas.1411762111, 2014.

Laskar, J., Robutel, P., Joutel, F., Gastineau, M., Correia, A., and Levrard, B.: A long-term numerical solution for the insolation quantities of the Earth, Astron. Astrophys., 428, 261–285, 2004.

Lisiecki, L. E.: Links between eccentricity forcing and the 100,000-year glacial cycle, Nat. Geosci., 3, 349–352, https://doi.org/10.1038/ngeo828, 2010.

375 Lisiecki, L. E. and Raymo, M. E.: A Pliocene-Pleistocene stack of 57 globally distributed benthic δ18O records, Paleoceanography, 20, 2005.

Liu, Z., Cleaveland, L., and Herbert, T.: Early onset and origin of 100-kyr cycles in Pleistocene tropical SST records, Earth Planet. Sc. Lett., 265, 703–715, https://doi.org/10.1016/j.epsl.2007.11.016, 2008.

MacAyeal, D. R.: Irregular oscillations of the West Antarctic ice sheet, Nature, 359, 29–32, https://doi.org/10.1038/359029a0, 1992.

Marshall, S. J. and Clark, P. U.: Basal temperature evolution of North American ice sheets and implications for the 100-kyr cycle, Geophysical
380 Res. Lett., 29, 67–1–67–4, https://doi.org/10.1029/2002GL015192, 2002.

Milankovitch, M.: Kanon der Erdbestrahlung und seine Anwendung auf das Eiszeitenproblem, Royal Serbian Academy Special Publication, 133, 1–633, 1941.

Oerlemans, J.: Model experiments on the 100,000-yr glacial cycle., Nature, 287, 430–432, https://doi.org/10.1038/287430a0, 1980.

Paillard, D.: The timing of Pleistocene glaciations from a simple multiple-state climate model, Nature, 391, 378–381,
385 https://doi.org/10.1038/3489, 1998.

Paillard, D.: Glacial cycles: toward a new paradigm, Rev. Geophys., 39, 325–346, https://doi.org/10.1029/2000RG000091, 2001.

Paillard, D.: Quaternary glaciations: from observations to theories, Quaternary Sci. Rev., 107, 11–24, https://doi.org/10.1016/j.quascirev.2014.10.002, 2015.

Paillard, D.: The Plio-Pleistocene climatic evolution as a consequence of orbital forcing on the carbon cycle, Clim. Past, 13, 1259–1267, https://doi.org/10.5194/cp-13-1259-2017, 2017.

Paillard, D. and Parrenin, F.: The Antarctic ice sheet and the triggering of deglaciations, Earth Planet. Sc. Lett, 227, 263–271, https://doi.org/10.1016/j.epsl.2004.08.023, 2004.

Paillard, D., Labeyrie, L., and Yiou, P.: Macintosh Program performs time-series analysis, Eos, Transactions, AGU, 77, 379–379, https://doi.org/10.1029/96EO00259, 1996.

Parrenin, F. and Paillard, D.: Amplitude and phase of glacial cycles from a conceptual model, Earth Planet. Sc. Lett., 214, 243–250, https://doi.org/10.1016/S0012-821X(03)00363-7, 2003.

Parrenin, F. and Paillard, D.: Terminations VI and VIII (∼ 530 and ∼ 720 kyr BP) tell us the importance of obliquity and precession in the triggering of deglaciations, Clim. Past, 8, 2031–2037, https://doi.org/10.5194/cp-8-2031-2012, 2012.

Peltier, W. R. and Marshall, S.: Coupled energy-balance/ice-sheet model simulations of the glacial cycle: A possible connection between terminations and terrigenous dust, J. Geophys. Res-atmos., 100, 14 269–14 289, https://doi.org/10.1029/95JD00015, 1995.

Pollard, D.: A simple ice sheet model yields realistic 100 kyr glacial cycles., Nature, 296, 334–338, https://doi.org/10.1038/296334a0, 1982.

Raymo, M.: The timing of major climate terminations, Paleoceanography, 12, 577–585, https://doi.org/10.1029/97PA01169, 1997.

Raymo, M. E. and Nisancioglu, K. H.: The 41 kyr world: Milankovitch's other unsolved mystery, Paleoceanography, 18, https://doi.org/10.1029/2002PA000791, 2003.

Saltzman, B. and Sutera, A.: The Mid-Quaternary Climatic Transition as the Free Response of a Three-Variable Dynamical Model, J. Atmos. Sci., 44, 236–241, https://doi.org/10.1175/1520-0469(1987)044<0236:TMQCTA>2.0.CO;2, 1987.

Saltzman, B., Hansen, A., and Maasch, K.: The Late Quaternary Glaciations as the Response of a Three-Component Feedback System to Earth-Orbital Forcing, J. Atmos. Sci., 41, 3380–3389, https://doi.org/10.1175/1520-0469(1984)041<3380:TLQGAT>2.0.CO;2, 1984.

Shackleton, N.: Oxygen Isotope Analyses and Pleistocene Temperatures Re-assessed, Nature, 215, 15–17, https://doi.org/10.1038/215015a0, 1967.

Shackleton, N. J. and Opdyke, N. D.: Oxygen isotope and palaeomagnetic stratigraphy of Equatorial Pacific core V28-238: Oxygen isotope temperatures and ice volumes on a 105 year and 106 year scale, Quaternary Res., 3, 39–55, https://doi.org/10.1016/0033-5894(73)90052-5, 1973.

Talento, S. and Ganopolski, A.: Evolution of the climate in the next million years: A reduced-complexity model for glacial cycles and impact of anthropogenic CO2 emissions, Earth Syst. Dynam. Discuss. [preprint], https://doi.org/10.5194/esd-2021-2, in review, 2021.

Toggweiler, J. R.: Origin of the 100,000-year timescale in Antarctic temperatures and atmospheric CO2, Paleoceanography, 23, https://doi.org/10.1029/2006PA001405, 2008.

Tzedakis, P., Crucifix, M., Mitsui, T., and Wolff, E. W.: A simple rule to determine which insolation cycles lead to interglacials, Nature, 542, 427–432, https://doi.org/10.1038/nature21364, 2017.

Tziperman, E. and Gildor, H.: On the mid-Pleistocene transition to 100-kyr glacial cycles and the asymmetry between glaciation and deglaciation times, Paleoceanography, 18, 1–1–1–8, https://doi.org/10.1029/2001pa000627, 2003.

Tziperman, E., Raymo, M. E., Huybers, P., and Wunsch, C.: Consequences of pacing the Pleistocene 100 kyr ice ages by nonlinear phase locking to Milankovitch forcing, Paleoceanography, 21, https://doi.org/10.1029/2005PA001241, 2006.

Yan, Y., Bender, M. L., Brook, E. J., Clifford, H. M., Kemeny, P. C., Kurbatov, A. V., Mackay, S., Mayewski, P. A., Ng, J., Sever-

425   inghaus, J. P., and Higgins, J. A.: Two-million-year-old snapshots of atmospheric gases from Antarctic ice, Nature, 574, 663–666,

https://doi.org/10.1038/s41586-019-1692-3, 2019.